Performance Analysis of In-building Small Cell Networks: Carrier Frequency Band Perspective

Rony Kumer Saha
Radio and Spectrum Laboratory
KDDI Research, Inc.
2-1-15 Ohara, Fujimino-shi, Saitama, Japan
email: ro-saha@kddi-research.jp

***Abstract*—In this paper, we present the performance of in-building small cells with the variation of carrier frequency from a low microwave band to a very high Terahertz (THz) band expected for the future Sixth-Generation (6G) mobile networks. We derive the average capacity, Spectral Efficiency (SE), Energy Efficiency (EE), and throughput per user of small cell networks. With extensive simulation results, we evaluate these performance metrics with a change in carrier frequency from a microwave band (i.e., 2 GHz), through a number of Millimeter-Wave (mmWave) bands (i.e., 28 GHz and 60 GHz), to a THz band (i.e., 140 GHz). It is shown that due to the presence of Line-of-Sight (LOS) components and availability of large spectrum bandwidth, the high-frequency mmWave and THz bands can play significant roles in improving the above performance metrics and achieve both SE and EE requirements expected for 6G mobile networks by reusing spectrum of their respective bands for a certain number of buildings of small cells.**

Keywords—6G; carrier frequency; path loss; in-building; small cell; millimeter-wave, spectrum reuse; THz band.

I. INTRODUCTION

A. Background

Exponentially increasing mobile traffic and high data rate demands, scarcity of the available radio spectrum, and limitations of the Base Station (BS) transmission power have caused Mobile Network Operators (MNOs) to move from large macrocell-only networks to Heterogeneous Networks (HetNets) [1]. In HetNets, small cells, typically deployed in indoor environments, cover a small area by reusing the spectrum bandwidth and play a significant role in serving high capacity and data rate within a short distance in mobile communication systems. To address the scarcity of available spectrum, the operating spectrum of small cells of one mobile generation shifts toward higher carrier frequencies than that of its predecessor one. As the signal propagation characteristics vary significantly with a change in carrier frequency, the performance of small cells also varies accordingly. This necessitates a deep understanding of how the channel performances within in-building environments vary with a change in the carrier frequency of small cells.

B. Related Work and Problem Statement

Numerous studies addressed the performance evaluation of small cells in multistory buildings, mostly in terms of signal propagation measurements, at different carrier frequencies. For example, the authors in [2] carried out propagation measurements in an indoor building environment at 900 MHz and 450 MHz. In [3], the authors presented a comparative study of two bands, below and above 6 GHz, including 3.5 GHz and 28 GHz. Further, in [4], the authors presented 28 GHz and 73 GHz millimeter-wave (mmWave) propagation measurements performed in a typical office environment. Furthermore, very recently, the authors in [5] performed channel measurements and path loss modeling in the Terahertz (THz) band.

Since the future Sixth-Generation (6G) network is expected to operate in low, as well as very high, frequency bands to address both coverage and capacity demands, instead of a certain frequency band discussed above, a common understanding of how the performance of small cells is affected with a change in the operating carrier frequency (and hence signal propagation characteristics) over a vast range, including very high THz band, is not obvious in the existing studies. To address this concern, in this paper, we present the performance analysis of in-building small cells over a vast range of carrier frequencies, from a low 2 GHz microwave band to a very high 140 GHz band for an efficient utilization of the spectrum in these bands.

In doing so, we consider a range of carrier frequencies that can cover the carrier frequencies of the former, existing, and upcoming mobile generations. More specifically, we start from a microwave band (i.e., 2 GHz used in the former Second-Generation (2G) up to Fourth-Generation (4G)), through a number of mmWave bands (i.e., 28 GHz used in the existing Fifth-Generation (5G) and 60 GHz expected to be used in the enhanced version of the existing 5G), to a THz band (i.e., 140 GHz) proposed to be used in the upcoming 6G mobile networks. However, due to a potential gap from one band to another of the above carrier frequencies, the channel characteristics in one band differ considerably from another. Hence, because of the occurrence of high small-scale fading effects, the Non-Line-of-Sight (NLOS) channel model for the 2 GHz microwave band, whereas the Line-of-Sight (LOS) channel model for the 28 GHz and 60 GHz mmWave bands and the 140 GHz band, are considered and given for a distance d in m in Table I.

C. Contribution

Based on the above discussion and consideration, in this paper, we contribute the following.

- We vary the carrier frequency of small cells from a low 2 GHz band to a very high 140 GHz band and derive the corresponding average capacity, Spectral Efficiency (SE),

 ISBN: 978-1-61208-837-2

Energy Efficiency (EE), and throughput per in-building small cell user performance metrics.

TABLE I. CHANNEL MODELS FOR DIFFERENT CARRIER FREQUENCY BANDS.

Channel Model			Value
Path loss	Carrier Frequency	2 GHz[1,2]	$127+30\log_{10}(d/1000)$
		28 GHz[5]	$61.38+17.97\log_{10}(d)$
		60 GHz[3]	$68+21.7\log_{10}(d)$
		140 GHz[4]	$75.89+21.17\log_{10}(d)$
Lognormal Shadowing standard deviation (dB)			10 (for 2 GHz)[1,2], 9.9 (for 28 GHz)[5], 0.88 (for 60 GHz)[3], and 0.5712 (for 140 GHz)[4]
Small-scale fading model			Frequency selective Rayleigh for 2 GHz[1], no small-scale fading effect for 28 GHz[5], 60 GHz[3], and 140 GHz[4]

taken [1]from [6], [2]from [7], [3]from [8], [4]from [5], [5]from [9].

- We carry out extensive simulation results and evaluate these performance metrics to show the significance of the variation in the operating carrier frequency on the performance of in-building small cell networks.
- Finally, we present a performance comparison against both SE and EE requirements expected for the 6G mobile networks by reusing the spectrum of each carrier frequency band for a certain number of buildings of small cells.

D. *Organization*

The paper is organized as follows. In Section II, we discuss the system architecture to evaluate the performance and derive performance metrics in terms of average capacity, Spectral Efficiency (SE), Energy Efficiency (EE), as well as average throughput per small cell user for all carrier frequencies. In Section III, performance evaluation scenarios are described, and extensive simulation results and performance comparisons are carried out. We draw a conclusion in Section IV.

II. System Architecture and Performance Metrics

A. *System Architecture*

We consider a simple system architecture for the performance evaluation as shown in Figure 1. A number of Picocell Base Stations (PBSs) are located outdoors, and all small cell BSs (SBSs) are located indoors within a number of buildings situated over the coverage of a Microcell Base Station (MBS). A number of Macrocell User Equipments (UEs) are considered indoors and all other outdoor Macrocell UEs (MUEs) are either served by the MBS or offloaded to nearby PBSs. However, all Small Cell UEs (SUEs) are served only by in-building SBSs. Both MBSs and PBSs operate in the 2 GHz band, whereas all SBSs operate at either 2 GHz, 28 GHz, 60 GHz, or 140 GHz band at any time.

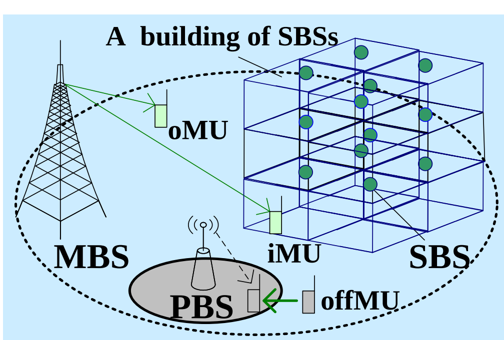

Figure 1. System architecture. oMU, iMU, and offMU define outdoor, indoor, and offloaded MUEs, respectively.

B. *Performance Metrics Estimation*

1) Preliminary: Let M_2, M_{28}, M_{60}, and M_{140} denote, respectively, the number of Resource Blocks (RBs) in the 2 GHz, 28 GHz, 60 GHz, and 140 GHz bands where an RB is equal to 180 kHz. Let M_{MC} denote the number of RBs in the 2 GHz band allocated exclusively to MBSs and PBSs, and hence is orthogonal to M_2 to avoid Co-Channel Interference (CCI) with SUEs. Let $P_{t,i}$, $N_{t,i}$, and $I_{t,i}$ denote, respectively, the transmission power, noise power, and total interference signal power at any RB *i* in Transmission Time Interval (TTI) *t*.

Using the formulas given in Table I, the path loss can be calculated for each carrier frequency. Let $PL_{t,i}$, $LS_{t,i}$, and $SS_{t,i}$ denote, respectively, the path loss, large-scale shadowing, small-scale fading between a SBS and an SUE at RB *i* in TTI *t*. Let (G_t+G_r) and L_F denote, respectively, the total antenna gain and connector loss such that a link channel response, denoted as $H_{t,i}$, between an SUE and a SBS at RB *i* in TTI *t* can be given by in dB as follows.

$$H_{t,i}(\text{dB}) = (G_t+G_r)-(L_F+PL_{t,i})+(LS_{t,i}+SS_{t,i}) \quad (1)$$

The received Signal-to-Interference-plus-Noise Ratio (SINR) for an SUE at RB *i* in TTI *t* can be expressed as follows.

$$\rho_{t,i} = \left(P_{t,i}/(N_{t,i}+I_{t,i})\right).H_{t,i} \quad (2)$$

Using Shannon's capacity formula, a link throughput at RB *i* in TTI *t* in bps per Hz is given by,

$$\sigma_{t,i}(\rho_{t,i}) = \begin{cases} 0, & \rho_{t,i} < -10\,\text{dB} \\ \beta\log_2\left(1+10^{(\rho_{t,i}(\text{dB})/10)}\right), & -10\,\text{dB} \le \rho_{t,i} \le 22\,\text{dB} \\ 4.4, & \rho_{t,i} > 22\,\text{dB} \end{cases} \quad (3)$$

where β denotes implementation loss factor.

The total capacity of all MUEs in $t\in\boldsymbol{T}=\{1,2,\ldots,Q\}$ is given by,

$$\sigma_{\text{MU}} = \sum_{t=1}^{Q}\sum_{i=1}^{M_{\text{MC}}}\sigma_{t,i}(\rho_{t,i}) \quad (4)$$

Now, the aggregate capacity served by a SBS in a building in $t\in\boldsymbol{T}$ over M_2 RBs is given by,

$$\sigma_s = \sum_{t\in\boldsymbol{T}}\sum_{i=1}^{M_2}\sigma_{t,i}(\rho_{t,i}) \quad (5)$$

Let S_F denote the number of SBSs per building. The aggregate capacity served by all SBSs in a single building when operating only in the 2 GHz band is then given by,

$$\sigma_{SU,2,L=1} = \sum_{s=1}^{S_F} \sigma_s \quad (6)$$

$$\sigma_{SU,2,L=1} = \sum_{s=1}^{S_F} \sum_{t \in \mathcal{T}} \sum_{i=1}^{M_2} \sigma_{t,i}\left(\rho_{t,i}\right) \quad (7)$$

2) Average capacity, SE, and EE: Let P_2, P_{28}, P_{60}, and P_{140} denote, respectively, the transmission power of a small cell when operating in the 2 GHz, 28 GHz, 60 GHz, and 140 GHz bands. P_M and P_P denote, respectively, the transmission power of an MBS and a PBS. Let S_M, S_P, and S_F denote, respectively the number of MBSs, PBSs, and SBSs per building. Because of the small coverage and low transmission power of a SBS, as well as low SUE speed, an indoor channel does not vary considerably within a short time such that we consider similar indoor signal propagation characteristics for all L buildings per macrocell.

Then, by linear approximation, the system-level average capacity per macrocell of the MNO is given by the sum of the aggregate capacity of all macrocell UEs and the aggregate capacity of all small cell UEs in L buildings. So, using (4) and (7), the system-level average capacity per macrocell is given by

$$\sigma_{2,L>1} = \sigma_{MU} + \left(L \times \sigma_{SU,2,L=1}\right) \quad (8)$$

Since SE is defined as the achievable capacity per unit of spectrum bandwidth, using (8), the system-level average SE in bps/Hz can be expressed as follows.

$$\gamma_{2,L>1} = \sigma_{2,L>1} \Big/ \left(\left(M_{MC} + M_2\right) \times Q\right) \quad (9)$$

Since EE can be defined as the amount of energy required to transmit a bit of information, using (8), the system-level EE in Joule/bit can be expressed as follows.

$$\varepsilon_{2,L>1} = \begin{pmatrix} \left(L \times S_F \times P_2\right) + \\ \left(S_M \times P_M + S_P \times P_P\right) \end{pmatrix} \Big/ \left(\sigma_{2,L>1} / Q\right) \quad (10)$$

3) Average throughput per SUE: Assume that each SBS can serve one SUE at any time in all carrier frequencies. The average throughput per SUE when SBSs operate in the 2 GHz band can then be expressed for S_F SBSs per building as follows.

$$\sigma_{2,s} = \sigma_{SU,2,L=1} / S_F \quad (11)$$

Following the above procedure and using (4)-(9) for the 2 GHz band, the system-level average capacity, SE, EE, and average throughput per SUE when small cells operate in the 28 GHz, 60 GHz, and 140 GHz can also be derived.

III. PERFORMANCE EVALUATION SCENARIO, RESULT, AND COMPARISON

A. *Performance Evaluation Scenario*

Default simulation parameters and assumptions for SBSs are given in Table II. For MBSs and PBSs, detailed parameters and assumptions can be found in [10]. Note that, for fair analysis, we consider the same parameters and assumptions, wherever applicable, including system bandwidth, symbol duration, transmission power, antenna configuration, and antenna gain of all SBSs and UEs, for all carrier frequencies even though they differ from one carrier frequency to another in practice. RBs of any band are allocated orthogonally to SBSs in any TTI by the Proportional Fair (PF) scheduler to avoid CCI between SBSs. Moreover, for simplicity, we assume that no CCI effect is experienced by any in-building SBS when operating in the 60 GHz band due to coexisting with the IEEE 802.11ad/ay, also termed as Wireless Gigabit (WiGig), access points.

Further, we assume that each MNO in a country is allocated to a dedicated spectrum in the 2 GHz, 28 GHz, and 140 GHz bands such that no CCI effect is experienced by any in-building SBS due to operating in the spectrum by SBSs of another MNO. Such CCI can be either avoided using techniques such as the time-domain Almost Blank Subframe based Enhanced Intercell Interference Coordination (eICIC) technique for Long Term Evolution (LTE) systems or mitigated using techniques such as the underlay cognitive radio spectrum access technique, which we consider out of the scope of this paper. Finally, we generate the performance results by simulating all assumptions and parameters given in Tables I and II by a simulator built using the computational tool MATLAB R2012b version running on a personal computer.

TABLE II. DEFAULT PARAMETERS AND ASSUMPTIONS

Parameters and Assumptions	Value
Transmit direction	Downlink
SBS operating bandwidth	50 MHz (for each carrier frequency)
Number of RBs in the SBS bandwidth	250 (for each carrier frequency)
Number of SBSs	48 (per building)
Transmission power (dBm)[7]	10 (for each carrier frequency)
Antenna configuration	Single-input single-output for all SBSs and SUEs
SBS antenna gain[7]	21 dB
SUE antenna gain[7] and noise figure	21 dB and 10 dB
Scheduler and traffic model[6]	Proportional Fair (PF) and full buffer
Type of SBSs	Closed Subscriber Group (CSG) femtocell BSs
Building and small cell models: Number of buildings, floors per building, apartments per floor, small cells per apartment, area of an apartment	 L, 6, 8, 1, 10×10 m^2
TTI[8] and scheduler time constant (t_c)	1 ms and 100 ms
Total simulation run time	8 ms

taken from [6]from [7], [7]from [5], [8]from [6].

B. *Performance Evaluation Result*

Figure 2(a) shows the path loss response for a SBS with the variation in distance d of its SUE. It can be found that the path loss at distance d from a SBS is the most when the SBS operates in the 140 GHz band, and the least, when it operates in the 2 GHz microwave band. In general, with an increase in the carrier frequency, the path loss increases since a high-frequency signal gets affected more by the propagating environment than that of a low-frequency one. This implies that to address high capacity and data rate demands of the future mobile networks, the availability of large spectrum bandwidth in the high-frequency bands such as THz bands will play a vital role in serving high capacity and data rate demands within a short indoor distance from a SBS.

Figure 2(b) shows the response of the average throughput per SUE in different carrier frequencies. It can be observed that, for LOS signal propagations in the high-frequency bands, the average throughput per SUE over a certain time T decreases with an increase in the carrier frequency. This is because an increase in carrier frequency causes to increase in the distant-dependent path loss as shown in Figure 2(a). However, the average throughput per SUE is the lowest when SBSs operate in the 2 GHz low-frequency band. This is due to the NLOS signal propagation that occurs from the presence of large multipath fading components in the low-frequency band unlike the high-frequency one with a LOS signal propagation as aforementioned.

Figures 3(a) and 3(b) show, respectively, the system-level SE and EE performances for the 10 MHz bandwidth of all MUEs. Recall that due to considering the LOS models, high-frequency signals offer high average capacity, as well as average throughput per SUE because of highly directive signal propagation toward SUEs such that by forming appropriate beam width, the enormous amount of average capacity and hence SE can be obtained. Moreover, due to an increase in average capacity, the average energy required per bit transmission is also reduced, resulting in improving EE as well.

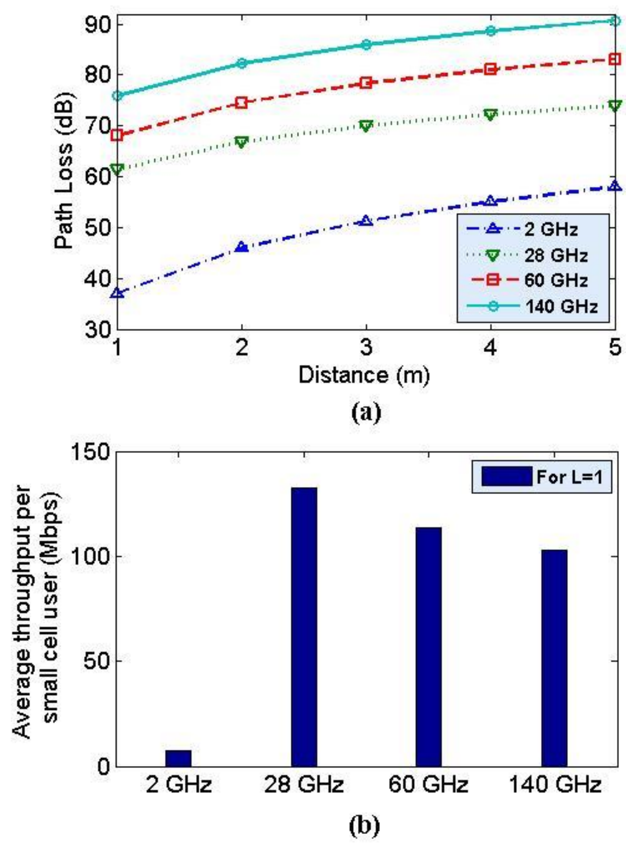

Figure 2. (a) Path loss and (b) average throughput per SUE responses with a variation in the carrier frequency of in-building SBSs.

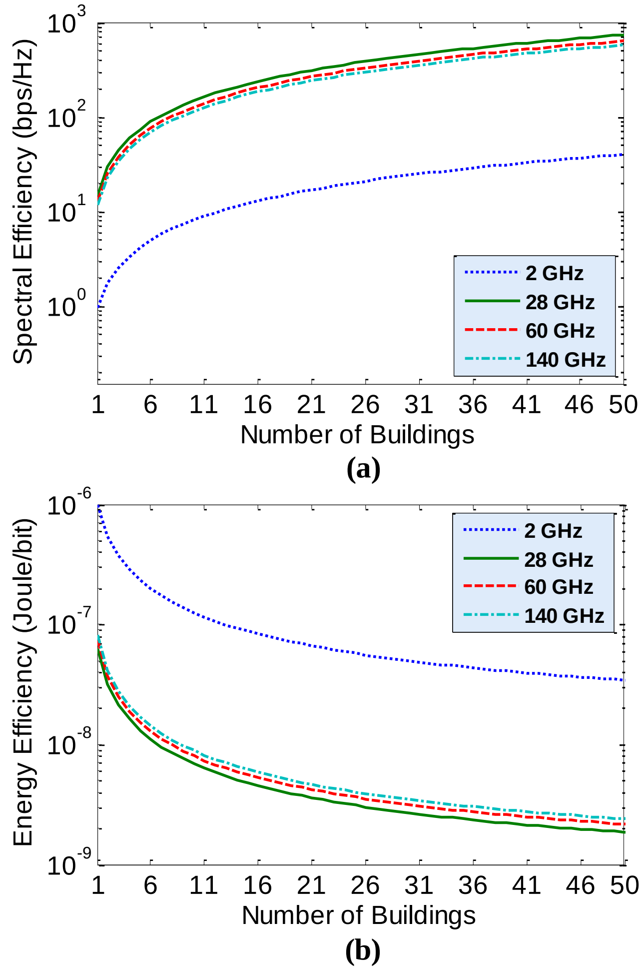

Figure 3. System-level performances with a variation in the carrier frequency of in-building SBSs. (a) spectral efficiency and (b) energy efficiency.

From Figure 2(a), since the path loss increases with an increase in LOS carrier frequency, the system-level SE and EE improve with a decrease in carrier frequency. Hence, the maximum and minimum improvements in both SE and EE are obtained when SBSs operate in the 28 GHz and 140 GHz bands, respectively. However, due to the NLOS signal propagation effect, the 2 GHz band provides the worst performance in the average capacity (Figure 2(b)), resulting in realizing the worst system-level SE and EE performances in NLOS 2 GHz carrier frequency as shown in Figures 3(a) and 3(b).

C. Performance Evaluation Comparison

Recall that unlike the low-frequency 2 GHz microwave band, which is affected considerably by the multipath fading effect from the reflection, refraction, and scattering phenomenon, due to the presence of LOS components and availability of large spectrum bandwidth, high carrier frequency bands can play significant roles in improving the in-building average throughput per SUE, as well as system-level average capacity, SE, and EE of the future mobile systems.

In this regard, assume that the prospective average SE and EE requirements for 6G mobile networks are, respectively, 10

ISBN: 978-1-61208-837-2

times (i.e., 370 bps/Hz) [11] and 10-100 times (i.e., 0.3µJ/bit - 0.03µJ/bit) [12] higher than that of 5G mobile networks [13]-[14]. From Figures 3(a) and 3(b), it can be found that all high carrier frequency bands, i.e., 28 GHz, 60 GHz, and 140 GHz, can achieve both SE and EE requirements expected for 6G mobile networks by reusing spectrum in their respective bands for a reuse factor (i.e., *L*) of 26, 30, and 33, respectively.

IV. CONCLUSION

Small cells deployed in indoor environments play a significant role in serving high capacity and data rate within a short distance in mobile communication systems. Due to the scarcity of spectrum, the operating spectrum of small cells of one mobile generation shifts toward higher carrier frequencies than that of its predecessor one. As the signal propagation characteristics vary significantly with a change in carrier frequency, in this paper, we have presented the performance of in-building small cells with the variation of carrier frequency from a low microwave band to a very high Terahertz (THz) band expected for the future Sixth-Generation (6G) mobile networks.

We have derived the average capacity, Spectral Efficiency (SE), Energy Efficiency (EE), and throughput per small cell UE (SUE) and carried out extensive simulation results with a change in carrier frequency from a microwave band (i.e., 2 GHz), through a number of millimeter-wave (mmWave) bands (i.e., 28 GHz and 60 GHz), to a THz band (i.e., 140 GHz). It has been shown that due to the presence of LOS components, high-frequency signals offer high average capacity and hence SE, as well as average throughput per SUE. Moreover, due to an increase in average capacity, the average energy required per bit transmission is also reduced, resulting in improving EE as well. Since the path loss increases with an increase in LOS carrier frequency, the maximum and minimum improvements in both SE and EE are obtained when SBSs operate in the 28 GHz and 140 GHz bands, respectively.

However, due to the NLOS signal propagation effect, the 2 GHz band is affected considerably by the multipath fading effect from the reflection, refraction, and scattering phenomenon such that the 2 GHz band provides the worst performance in the average capacity. This results in achieving the worst system-level SE and EE performances. Finally, it has been shown that all high carrier frequency bands, i.e., 28 GHz, 60 GHz, and 140 GHz, can achieve both SE and EE requirements expected for 6G mobile networks by reusing spectrum in their respective bands for a reuse factor (i.e., *L*) of 26, 30, and 33, respectively.

REFERENCES

[1] D. López-Pérez, M. Ding, H. Claussen, and A. H. Jafari, “Towards 1 Gbps/UE in Cellular Systems: Understanding Ultra-Dense Small Cell Deployments,” IEEE Communications Surveys & Tutorials, vol. 17, no. 4, pp. 2078-2101, Fourthquarter 2015, doi: 10.1109/COMST.2015.2439636.

[2] A. Chandra, “Comparative Study of 900 MHz and 450 MHz Radio Signals Propagation in an Indoor Environment,” Proc. 1996 IEEE International Conference on Personal Wireless Communications Proceedings and Exhibition. Future Access, New Delhi, India, 1996, pp. 247-253, doi: 10.1109/ICPWC.1996.494278.

[3] A. M. Al-Samman et al., “Comparative Study of Indoor Propagation Model Below and Above 6 GHz for 5G Wireless Networks. Electronics, vol 8, no. 44, 2019. doi:10.3390/electronics8010044

[4] S. Deng, M. K. Samimi, and T. S. Rappaport, ‘28 GHz and 73 GHz millimeter-wave Indoor Propagation Measurements and Path Loss Models,” Proc. 2015 IEEE International Conference on Communication Workshop (ICCW), London, UK, 2015, pp. 1244-1250, doi: 10.1109/ICCW.2015.7247348.

[5] N. A. Abbasi, A. Hariharan, A. M. Nair, and A. F. Molisch, “Channel Measurements and Path Loss Modeling for Indoor THz Communication,” Proc. 2020 14th European Conference on Antennas and Propagation (EuCAP), Copenhagen, Denmark, 2020, pp. 1-5, doi: 10.23919/EuCAP48036.2020.9135643.

[6] 3GPP. *Evolved Universal Terrestrial Radio Access (E-UTRA); Radio Frequency (RF) System Scenarios. Document 3GPP TR 36.942, V.1.2.0, 3rd Generation Partnership Project, Jul. 2007.* [online] Available from: https://portal.3gpp.org/ desktopmodules /Specifications/Specification Details.aspx?specificationId=2592 [retrieved February, 2020]

[7] *Simulation Assumptions and Parameters for FDD HeNB RF Requirements. document TSG RAN WG4 (Radio) Meeting #51, R4-092042, 3GPP, May 2009*. [online] Available from: https://www.3gpp.org/ftp/tsg_ran /WG4_Radio/TSGR4_51 /Documents/ [retrieved February, 2020].

[8] S. Geng, J. Kivinen, X. Zhao, and P. Vainikainen, “Millimeter-Wave Propagation Channel Characterization for Short-Range Wireless Communications,” IEEE Transactions on Vehicular Technology, vol. 58, no. 1, pp. 3-13, Jan. 2009, doi: 10.1109/TVT.2008.924990.

[9] G. R. Maccartney, T. S. Rappaport, S. Sun, and S. Deng, “Indoor Office Wideband Millimeter-Wave Propagation Measurements and Channel Models at 28 and 73 GHz for Ultra-Dense 5G Wireless Networks,” IEEE Access, vol. 3, pp. 2388-2424, 2015, doi: 10.1109/ACCESS.2015.2486778

[10] R. K. Saha, “3D Spatial Reuse of Multi-Millimeter-Wave Spectra by Ultra-Dense In-Building Small Cells for Spectral and Energy Efficiencies of Future 6G Mobile Networks,” Energies, vol. 13, no. 7, 1748, pp.1-19, 2020. doi: 10.3390/EN13071748

[11] Z. Zhang et al., “6G Wireless Networks: Vision, Requirements, Architecture, and Key Technologies,” IEEE Vehicular Technology Magazine, vol. 14, no. 3, pp. 28-41, Sept. 2019, doi: 10.1109/MVT.2019.2921208.

[12] S. Chen et al. , “Vision, Requirements, and Technology Trend of 6G: How to Tackle the Challenges of System Coverage, Capacity, User Data-Rate and Movement Speed,” IEEE Wireless Communications, vol. 27, no. 2, pp. 218-228, April 2020, doi: 10.1109/MWC.001.1900333.

[13] C. Wang et al., “Cellular architecture and Key Technologies for 5G Wireless Communication Networks,” IEEE Communications Magazine, vol. 52, no. 2, pp. 122-130, February 2014, doi: 10.1109/MCOM.2014.6736752.

[14] G. Auer et al., “How much energy is needed to run a wireless network?,” IEEE Wireless Communications, vol. 18, no. 5, pp. 40-49, October 2011, doi: 10.1109/MWC.2011.6056691.